



Enhanced nitrogen diffusion induced by atomic attrition

E. A. Ochoa, C. A. Figueroa, T. Czerwiec, and F. Alvarez

Citation: [Applied Physics Letters](#) **88**, 254109 (2006); doi: 10.1063/1.2216032

View online: <http://dx.doi.org/10.1063/1.2216032>

View Table of Contents: <http://scitation.aip.org/content/aip/journal/apl/88/25?ver=pdfcov>

Published by the [AIP Publishing](#)

Articles you may be interested in

[Influence of crystal orientation and ion bombardment on the nitrogen diffusivity in single-crystalline austenitic stainless steel](#)

J. Appl. Phys. **110**, 074907 (2011); 10.1063/1.3646493

[Anisotropic ion-enhanced diffusion during ion nitriding of single crystalline austenitic stainless steel](#)

J. Appl. Phys. **105**, 093502 (2009); 10.1063/1.3120912

[Ion beam nitriding of single and polycrystalline austenitic stainless steel](#)

J. Appl. Phys. **97**, 083531 (2005); 10.1063/1.1863455

[Chemical state of nitrogen in a high nitrogen face-centered-cubic phase formed on plasma source ion nitrided austenitic stainless steel](#)

J. Vac. Sci. Technol. A **22**, 2067 (2004); 10.1116/1.1786305

[Chemical bonding of nitrogen in low energy high flux implanted austenitic stainless steel](#)

J. Appl. Phys. **91**, 6361 (2002); 10.1063/1.1469691



AIP | Journal of
Applied Physics

Journal of Applied Physics is pleased to
announce **André Anders** as its new Editor-in-Chief

Enhanced nitrogen diffusion induced by atomic attrition

E. A. Ochoa, C. A. Figueroa, T. Czerwiec,^{a)} and F. Alvarez^{b)}

Instituto de Física “Gleb Wataghin,” Universidade Estadual de Campinas, Unicamp 13083-970, Campinas, São Paulo, Brazil

(Received 4 March 2006; accepted 22 May 2006; published online 23 June 2006)

The nitrogen diffusion in steel is enhanced by previous atomic attrition with low energy xenon ions. The noble gas bombardment generates nanoscale texture surfaces and stress in the material. The atomic attrition increases nitrogen diffusion at lower temperatures than the ones normally used in standard processes. The stress causes binding energy shifts of the Xe $3d_{5/2}$ electron core level. The heavy ion bombardment control of the texture and stress of the material surfaces may be applied to several plasma processes where diffusing species are involved. © 2006 American Institute of Physics. [DOI: 10.1063/1.2216032]

The properties of materials obtained in several applications involving plasma such as plasma enhanced deposition, ion beam assisted deposition, and pulsed plasma nitriding are directly influenced by the defects at the surface created by the impact of ions. Modern plasma nitriding combines low energy nitrogen ion implantation and posterior thermal diffusion.^{1,2} Plasma nitriding is a broadly used thermochemical diffusion process increasing hardness and corrosion resistance, and improving tribological properties of iron based alloys. However, diminishing the relative long processing times continues to be a challenge for increasing applications of the process. The synergy between low energy ions and substrate temperature influencing kinetic surface phenomena recently demonstrated is an important route of working to decrease process time.³ Mechanical attrition (“shot peening”) generating plastic deformation and defects modifies the surface chemical kinetic of the reactions, shortening nitriding process by increasing boundary paths obtained in the nanostructured surface.^{4–7} Recently, Abrasonis *et al.* showed nitriding enhancement in steel by ion argon postbombardment treatments.⁸ These researches proposed a mechanism involving nonlinear elemental vibration excitation as the cause of the observed phenomenon.

In this letter we report that the preparation of the surface samples by low energy xenon ion bombardment (“atomic attrition”) and posterior *in situ* nitriding process notably enhances nitrogen diffusion. This result allows lowering temperature process or shortening nitriding times, two important variables. Although less intense, similar results were obtained using krypton ions. In this letter, however, we shall focus the discussion on the experiments performed with Xe⁺ bombardment. *In situ* photoemission electron spectroscopy (XPS) shows that the low energy (from 50 to 350 eV) implanted Xe⁺ generates local stress (“atomic peening”).^{9,10} The local stress was studied investigating the binding energy shifts of the Xe $3d_{5/2}$ electron core level due to the pressure exerted on the trapped noble gas by the host crystalline structure. *Ex situ* field emission gun scanning electron microscopy (FEG-SEM) shows that the Xe⁺ bombardment generates na-

nometric fine grains at the material surface, augmenting diffusion paths. *Sputtered neutral mass spectroscopy* (SNMS) shows enhancing nitrogen diffusion in previously Xe⁺ bombarded substrates. Grazing angle diffractograms show a remarkable increasing of species rich in nitrogen. These physical modifications lead to a more efficient nitriding process, increasing the material hardness. Finally, our findings combined with the results reported by Abrasonis *et al.* suggest that the effect of bombarding the material before as well as after nitriding has profound consequences on N diffusion in metals.⁸

The experiments were performed in mirror polished, rectangular samples, 20×10 mm, 1 mm thick, prepared from the same commercial AISI 4140 steel lot (C: 0.4, Si: 0.25, P: <0.04, S: <0.04, Mn: 0.85, Mo: 0.20, Cr: 1, Fe: balance). The Xe⁺ implantation and nitriding experiments were carried out in a high-vacuum system (<10⁻⁷ mbar) attached to an ultrahigh-vacuum chamber (<2×10⁻⁹ mbar) for XPS analysis. The deposition chamber contains a 3 cm diameter dc Kaufman ion source. Details of the apparatus are described elsewhere.¹¹ Before nitriding, the surface of the samples is nanostructured by Xe⁺ bombardment for 30 min at room temperature with energies varying between 50 and 350 eV and ion current density of 1 mA/cm². Immediately, the substrate temperature is raised to the working nitriding temperature (380±5) °C in approximately 15 min. Subsequently, the sample is irradiated with a pure nitrogen ion beam of 1 mA/cm² and constant energy (200 eV) for all the studied samples. Two sets of samples were prepared by irradiating the substrate for 30 min and 120 min, respectively. The treated sample is then transferred to the XPS analysis chamber. The hardness profiles were obtained by nanoindentation using a Berkovich diamond tip (NanoTest-300) and the load-displacement curves were analyzed by the Oliver and Pharr method.¹² The nitrogen profiles were obtained from SNMS. The nitrogen concentration was obtained using a γ' -Fe₄N standard sample. The sample cross-section morphology was studied by FEG-SEM (10 s attack with a 5% nital solution). The crystalline structure was studied by normal and glazing x-ray experiments. Numerical simulation using TRIM shows that the Xe depth in the studied samples varies between ~5 and 40 Å depths.¹³ This is the region probed by the XPS technique.¹⁴ The [Xe]/[Fe] ratio in all treated samples is ~1.3±0.1 at. % as obtained by XPS.

Figure 1(a) shows the hardness profiles of the nitrided

^{a)}Also at Laboratoire de Science et Genie des Surfaces (UMR CNRS 7570), Institut National Polytechnique de Lorraine, Ecole des Mines de Nancy, Parc de Saurupt, 54042 Nancy Cedex, France.

^{b)}Author to whom correspondence should be addressed; electronic mail: alvarez@if.unicamp.br

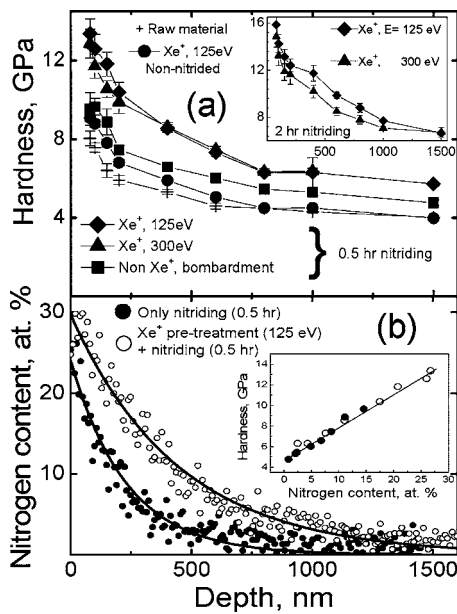


FIG. 1. (a) Hardness vs depth. Crosses: raw material. Dots: sample sole bombarded with Xe⁺ ions. Squares: nitrided samples without xenon bombardment pretreatment. Triangles and diamonds: nitrided samples pretreated with Xe⁺. The energies of the xenon ions are indicated. Inset: Hardness vs depth of nitrided samples pretreated with Xe⁺ and longer process time. (b) Nitrogen depth profile of two nitrated samples with and without bombardment of 125 eV Xe⁺. Inset: hardness vs N concentration of the same samples. The nitriding times are indicated.

samples *in identical conditions* but different Xe⁺ bombarding preparation of the substrates. For comparison purposes, the hardness profiles of a sole Xe⁺ bombarded (non-nitrided) and raw samples are displayed. The increasing hardness at the surface of the raw material is explained by the bond order loss at the boundary sample and the polishing procedure.¹⁵ Figure 1(a) inset shows results obtained for longer nitriding time. Figure 1(b) shows the nitrogen profile obtained by SNMS of two nitrated samples with and without bombardment (125 eV Xe⁺). Figure 1(b) inset shows a linear relationship between hardness and nitrogen concentrations of these two samples.¹⁶ Figure 1(a) shows a small hardness increasing in the sample treated (only) with Xe⁺. TRIM simulation shows that the ion penetration for Xe 125 eV ions is ~ 10 Å (not shown). Therefore, the dislocations and defects causing the hardness increment propagate as far as ~ 700 nm. This “long range” phenomenon is a known effect.¹⁷ The preparation of the substrate by Xe⁺ bombardment enhances nitrogen diffusion efficiency, increasing hardening (Fig. 1). For relative short nitriding time (0.5 h), the curves for 125 and 300 eV are overlapping. Increasing nitriding time splits the hardness curves [Fig. 1(a) inset].

Figure 2 shows the grazing angle diffractograms obtained in a selected group of studied samples. The peak associated with ϵ -Fe₂₋₃N nitrides confirms the increasing retention of nitrogen at the surface in Xe⁺ bombarded samples. Bulk diffractograms (not shown) indicate the formation of γ' -Fe₄N and ϵ -Fe₂₋₃N phases, confirming N deeper diffusion. Assuming a diffusion parabolic law, the ~ 8 GPa hardness, for instance, could be reached approximately nine times faster by previous atomic attrition of the substrate (Fig. 1).¹⁸ The shifting of the diffraction peak is probably due to the network distortion occasioned by the ion bombardment (stress).

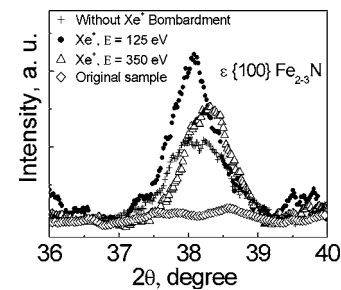


FIG. 2. Grazing angle diffractograms of the peak associated with ϵ -Fe₂₋₃N of nitrided samples. The bombarded Xe⁺ energies are indicated.

The Xe/Fe atomic ratio size is ~ 1.7 . In the same units, the-sizes of the largest α (bcc) interstitial sites in Fe are ~ 0.37 (tetrahedral) and 0.19 (octahedral), respectively.¹⁹ Let us assume for simplicity that, after a few collisions, the Xe atoms occupy an interstitial site in the α (bcc) host crystal, causing stress. The increasing volume in the plane of the nitrided layer is prevented from expanding due to the stiffness of the substrate.^{20,21} Therefore, due to the pressure caused by the misfitting atoms in the host crystal, the binding energy (BE) of the Xe 3d_{5/2} electron changes.^{22,23} Our results show BE changes of the Xe 3d_{5/2} core level up to -5 eV compared with the value measured in the free Xe atom (gas). This BE shift stems from the initial and final electronic states of the photoejected electron.^{22,24} The initial state contribution to the BE shift is essentially due the increasing electron repulsion introduced by the compression of the electronic cloud charge. The final state contribution to the BE shift relies on the network relaxation energy (RE) due to the hole left behind by the photoejected electron. Therefore, subtracting the RE from the Xe 3d_{5/2} peak energy shift will provide the true energy, ΔE , associated with the Fe host crystal compression effect on Xe. Experimentally, the RE can be obtained using the Auger parameter α .^{22,25,26} Briefly, the Auger parameter is determined by $\alpha = K + BE$, where K and BE are the kinetic energy of the Auger electron and the binding energy of the considered electronic level, respectively. The RE is then determined by the expression $RE \approx \alpha/2(14)$. Figure 3 shows the energy shift ΔE of the Xe 3d_{5/2} electron core level energies (after subtracting the RE) versus the ion implantation energy of the studied samples. As observed, a local maximum occurs at ~ 125 eV. Above this energy, the energy shift diminishes due to plastic relaxation of the material. A similar curve with a maximum located at ~ 150 eV is obtained by bombarding with Kr atoms (not shown). In this case, however, the maximum shift of the Kr 3p_{3/2} electron

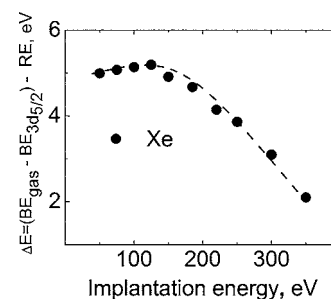


FIG. 3. Experimental binding energy shifts ΔE of the Xe 3d_{5/2} electron core levels (relative to the gas phase) minus the relaxation energy (RE) of the system vs implantation energy.

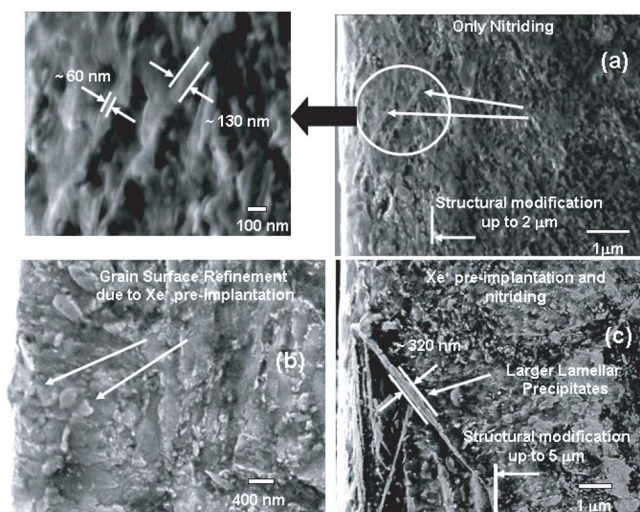


FIG. 4. (Color online) (a) SEM micrograph showing the nitrided layer in a substrate without Xe^+ preimplantation, (b) surface refinement due to the Xe^+ bombardment (125 eV), and (c) nitrided sample in a Xe^+ preimplanted sample.

core level is around 25% less than the shift obtained with the $\text{Xe } 3d_{5/2}$ electron core level energy.

Figure 4(a) shows the morphology of the nitrided layer without Xe^+ bombardment. The structural modification reaches up to $2 \mu\text{m}$ depth with lamellar precipitates. The detail (left) shows 60–130 nm size characteristic structures. The refining grain up to nanometric scale by Xe^+ bombardment creates numerous alternative paths for nitrogen diffusion [Fig. 4(b)].^{27,28} The micrograph of the nitrided Xe^+ bombardment sample shows a pattern formed by larger lamellar nitrogen precipitates, deeper in the sample, than the ones observed in Fig. 4(a), effect induced by the Xe^+ bombardment [Fig. 4(c)].

In conclusion, the preparation of the surface material by Xe^+ bombardment enhances nitrogen diffusion by grain refining up to nanometric dimensions. Therefore, the nitriding time is shortened and the process temperatures reduced. The atomic attrition generates stress as a consequence of the energy transferred by the impact and occupancy of small spaces by the massive Xe^+ ions (misfitting). Even though less intense, similar effects are observed using Kr^+ .

This work was partially sponsored by Fapesp. One of the authors (F.A.) is a CNPq fellow. Two of the authors (E.A.O. and C.A.F.) are Fapesp fellows. The authors are indebted to H. Michel and E. J. Mittemeijer for critical reading of the letter. This work is part of the EAO Ph.D. dissertation.

- ¹R. Wei, *Surf. Coat. Technol.* **83**, 218 (1996).
- ²T. Czerwiec, H. Michel, and E. Bergman, *Surf. Coat. Technol.* **108–109**, 102 (1998); K. T. Rie, E. Menthe, A. Matthews, K. Legg, and J. Chin, *MRS Bull.* **21**, 46 (1996).
- ³Z. Wang and E. G. Seebauer, *Phys. Rev. Lett.* **95**, 015501 (2005).
- ⁴W. P. Tong, N. R. Tao, Z. B. Wang, J. Lu, and K. Lu, *Science* **299**, 686 (2003).
- ⁵C. C. Koch, *Nanostruct. Mater.* **2**, 109 (1993).
- ⁶C. Suryanarayana, *Prog. Mater. Sci.* **46**, 1 (2001).
- ⁷Q. Jiang, S. H. Zhang, and J. C. Li, *Solid State Commun.* **130**, 581 (2004).
- ⁸G. Abrasonis, W. Möller, and X. Ma, *Phys. Rev. Lett.* **96**, 065901 (2006).
- ⁹C. A. Davis, *Thin Solid Films* **226**, 30 (1993).
- ¹⁰H. Windischmann, *J. Appl. Phys.* **62**, 1800 (1987).
- ¹¹P. Hammer, N. M. Victoria, and F. Alvarez, *J. Vac. Sci. Technol. A* **16**, 2941 (1998).
- ¹²W. C. Oliver and G. M. Pharr, *J. Mater. Res.* **7**, 1564 (1992).
- ¹³J. P. B. Biersack and G. L. Haggmark, The simulation used the TRIM software. *Nucl. Instrum. Methods* **174**, 257 (1980).
- ¹⁴See *Practical Surface Analysis*, 2nd ed., edited by D. Briggs and M. P. Seah (Wiley, New York, 1996), Vol. 1.
- ¹⁵C. Q. Sun, W. H. Zhon, S. Li, and B. K. Tay, *J. Phys. Chem. B* **108**, 1080 (2004).
- ¹⁶E. A. Ochoa, C. A. Figueroa, and F. Alvarez, *Surf. Coat. Technol.* **200**, 2165 (2005).
- ¹⁷Yu. P. Sharkeev and E. V. Kozlov, *Surf. Coat. Technol.* **158–159**, 219 (2002), and references therein.
- ¹⁸W. D. Callister, Jr., *Materials Science and Engineering. An Introduction*, 5th ed. (Wiley, New York, 2000).
- ¹⁹R. W. K. Honeycombe and H. K. D. H. Bhadeshia, *Steels, Microstructure and Properties* (Edward Arnold, London, 1995).
- ²⁰J. D. Kamminga, Th. H. de Keijser, and R. Delhez, *J. Appl. Phys.* **11**, 6332 (2000).
- ²¹J. D. Kamminga, Th. H. de Keijser, R. Delhez, and E. J. Mittemeijer, *Thin Solid Films* **317**, 169 (1998).
- ²²P. H. Citrin and D. R. Haman, *Phys. Rev. B* **10**, 4948 (1974).
- ²³R. G. Lacerda, M. C. dos Santos, L. R. Tessler, P. Hammer, F. Alvarez, and F. C. Marques, *Phys. Rev. B* **68**, 054104 (2003).
- ²⁴Y. Baba, H. Yamamoto, and T. A. Sasaki, *Surf. Sci.* **287/288**, 806 (1993).
- ²⁵C. D. Wagner, *Faraday Discuss. Chem. Soc.* **60**, 291 (1975).
- ²⁶G. Moretti, *J. Electron Spectrosc. Relat. Phenom.* **95**, 95 (1998).
- ²⁷R. E. Reed-Hill, *Physical Metallurgy Principles*, 2nd ed. (Van Nostrand, New York, 1973).
- ²⁸Q. Jiang, S. H. Zhang, and J. C. Li, *Solid State Commun.* **130**, 581 (2004).